Conversion of human fibroblasts into angioblast-like multipotent progenitor cells

Leo Kurian[1,*], **Ignacio Sancho-Martinez**[1,*], **Emmanuel Nivet**[1,*], **Aitor Aguirre**[1], **Krystal Moon**[1], **Caroline Pendaries**[2], **Cecile Volle-Challier**[2], **Francoise Bono**[2], **Jean-Marc Herbert**[2], **Julian Pulecio**[3], **Yun Xia**[1], **Mo Li**[1], **Nuria Montserrat**[3], **Sergio Ruiz**[1], **Ilir Dubova**[1], **Concepcion Rodriguez**[1], **Ahmet M. Denli**[4], **Francesca S. Boscolo**[5], **Rathi D. Thiagarajan**[5], **Fred H. Gage**[4], **Jeanne F. Loring**[5,6], **Louise C. Laurent**[5,7], and **Juan Carlos Izpisua Belmonte**[1,3]

[1]Gene Expression Laboratory, Salk Institute for Biological Studies, 10010 North Torrey Pines Road, La Jolla, CA 92037 USA

[2]Sanofi-Aventis R&D, E2C, 195 Route d'fEspagne, Toulouse Cedex 31636, France

[3]Center of Regenerative Medicine in Barcelona, Dr. Aiguader, 88, 08003 Barcelona, Spain

[4]Laboratory of Genetics, Salk Institute for Biological Studies, 10010 North Torrey Pines Road, La Jolla, CA 92037 USA

[5]Department of Chemical Physiology, The Scripps Research Institute, La Jolla, CA 92037, USA

[6]Center for Regenerative Medicine, The Scripps Research Institute, La Jolla, CA 92037, USA

[7]Department of Reproductive Medicine, University of California, La Jolla, CA 92093, USA

Abstract

Lineage conversion of one somatic cell type into another constitutes an attractive approach for research and clinical use. Lineage conversion can proceed in a direct manner, in the absence of proliferation and multipotent progenitor generation, or in an indirect manner, by the generation of expandable multipotent progenitor states. Here we report on the development of a combined reprogramming methodology that, transitioning through a plastic intermediate state, allows for the generation of human mesodermal progenitor cells while circumventing the traditional hallmarks of pluripotency. Converted mesodermal progenitor cells demonstrated bi-potent differentiation potential and were able to generate endothelial and smooth muscle lineages. Importantly, human fibroblasts can be converted into angioblast-like progenitor cells by non-integrative approaches. Differentiated angioblast-like cells exhibit neo-angiogenesis and anastomosis *in vivo*. The

Author for correspondence: Juan Carlos Izpisua Belmonte, belmonte@salk.edu; izpisua@cmrb.eu.
*These authors contributed equally to this work

methodology for indirect lineage conversion to angioblast-like cells described here adds to the armamentarium of reprogramming approaches aimed at the clinical treatment of ischemic pathologies.

INTRODUCTION

Somatic cell reprogramming has highlighted the high plasticity of adult somatic cells as well as the possibility of generating any desired cell type in unlimited amounts. Based on the forced expression of selected transcription factors (TFs), three major different approaches allowing for somatic cell reprogramming have recently been described[1]. First, somatic cells can be reprogrammed into induced Pluripotent Stem Cells (iPSCs), embryonic-like cells with the potential, upon further differentiation, to generate all different cell-types present in the adult organism[2]. Second, the concept of TFs defining or specifying target cell identity has proven successful for the direct lineage conversion of mouse and human cells into a number of different cell types[3–6]. Finally, the fact that reprogramming leading to iPSC formation proceeds in a step-wise de-differentiation manner suggests that this process can be controlled and stopped prior to the acquisition of an embryonic-like signature. Indeed, coupling a partially de-differentiated plastic state to specific differentiation conditions has demonstrated a feasible alternative way to generate murine cardiac and neuronal cells[7–11].

In here we present the development of a simple and highly efficient method allowing for the conversion of human fibroblasts into CD34+ progenitor cells with bi-potent differentiation potential. The process of conversion occurs indirectly by shortening and/or bypassing complete reprogramming to pluripotency while allowing for the generation of a "plastic" state. Transitioning through a plastic intermediate state allowed for re-differentiation into CD34+ progenitor cells and subsequently, further differentiation to functional endothelial and smooth muscle lineages.

RESULTS

Development of an Angioblast-like differentiation media

We speculated that coupling a robust differentiation protocol to partially reprogrammed cells could provide a suitable platform for cell fate conversion. As such, we developed a robust media suitable for the differentiation of pluripotent stem cells (PSCs) to mesodermal progenitor cells prior to establishing the reprogramming conditions necessary for cell-fate conversion. Thus, we systematically analyzed different well-known mediators of mesodermal development in different human PSC (hPSC) lines[12]. We found that a media, hereafter referred to as Mesodermal Induction Media or MIM, containing DMEM:F12, 15 mg ml^{-1} stem cell grade BSA, 17.5 μg ml^{-1} Human Insulin, 275 μg ml^{-1} Human holo-transferrin, 20 ng ml^{-1} bFGF, 50 ng ml^{-1} Human VEGF, 25 ng ml^{-1} human BMP4, 450 μM monothioglycerol and 2.25 mM L-Glutamine and Non-essential amino acids, but in the absence of Activin-A, was highly efficient in driving hPSCs to a mesodermal fate (Fig. 1a and Supplementary Fig. 1). Next, we tested MIM differentiation on multiple human PSC lines by focusing on CD34 expression, an early marker for mesoderm-derived progenitor cells with hematopoietic and/or endothelial and smooth muscle differentiation potential (Fig.

1b–f and Supplementary Fig. 1–2). A peak of CD34+ cells was observed by day 8 in every analyzed cell line. In parallel, we observed upregulation of the vascular marker CD31 (Fig. 1b–f and Supplementary Fig. 1–2) accompanied by rapid downregulation of pluripotency-related markers (Fig. 1g and Supplementary Fig. 2). Similarly, expression of mesodermal progenitor markers was significantly upregulated (Fig. 1b–g and Supplementary Fig. 1–2). Additionally, we observed the upregulation of several early markers related to hematopoiesis, including *RUNX1* and *SCL/TAL1* (Supplementary Fig. 2). Thus, MIM might lead to the generation of a tri-potent hemangioblast-like state with hematopoietic, endothelial and smooth muscle differentiation potential. MIM-differentiated PSC-derived CD34+ cells ($_{PSC}$CD34+) did not result in the expression of any hematopoietic marker analyzed at the protein level or the formation of hematopoietic colonies in standard hematopoietic Colony Forming Assays.

We next wondered whether MIM-induced CD34+ cells represented a developmental stage similar to that of angioblast cells[13] by investigating the potential of $_{PSC}$CD34+ cells to differentiate into endothelial and smooth muscle lineages. Sorting of 8 days MIM-differentiated $_{PSC}$CD34+ cells and subsequent differentiation towards the endothelial lineage gave rise to endoglin and VE-cadherin positive endothelial cells (Fig. 1h and Supplementary Fig. 3). Importantly, expression of von Willebrand factor (vWF), a mature endothelial marker and pro-coagulant protein additionally playing a role in wound healing and vessel repair, was readily detected (Fig. 1h and Supplementary Fig. 3). Two-step differentiation of PSCs by inducing mesoderm commitment and subsequent differentiation of CD34+ cells towards the endothelial lineage, gave rise to 60–90% VE-cadherin+ endoglin+ cells in all cell lines analyzed. qPCR analysis of PSC-differentiated endothelial cells demonstrated significant upregulation of endothelial markers whereas no upregulation was observed for smooth muscle markers (Fig. 1i and Supplementary Fig. 3); thus, indicating specificity of differentiation towards the endothelial lineage.

Similarly, $_{PSC}$CD34+ cells were sorted and subjected to smooth muscle differentiation conditions. Differentiation of isolated progenitors yielded a high number of smooth muscle cells (Supplementary Fig. 4). mRNA analysis demonstrated significant upregulation of smooth muscle markers, including expression of the smooth muscle-specific high molecular weight Caldesmon type 1 (*CALD1*), while no endothelial marker was upregulated (Supplementary Fig. 4). Single cell differentiation assays demonstrated the multipotent nature of the generated cells (Supplementary Fig. 4). Next, we performed genome-wide DNA methylation and gene expression studies. As expected there was a clear distinction between all of the differentiated samples and the undifferentiated PSCs at both, the transcriptome as well as the methylome level (Fig. 1j, k and Supplementary Fig. 5). Few unique differences between PSC-endothelial differentiated cells and primary endothelial cells were found. Similarly, there was a clear distinction between all of the differentiated smooth muscle samples as compared to undifferentiated PSCs (Supplementary Fig. 6).

In summary, our studies identify a novel chemically defined media (MIM) leading to the generation of CD34+ progenitor cells in a more efficient manner than previously described protocols[14–16]. MIM differentiation was sufficient for the generation of $_{PSC}$CD34+ cells with the potential to generate both endothelial and smooth muscle lineages. Thus, MIM

differentiation of PSCs results in the generation of a progenitor population resembling an angioblast-like state.

Conversion of human fibroblasts to Angioblast-like cells

We next asked whether MIM could suffice for the conversion of human fibroblasts into CD34+ angioblast-like progenitor cells ($_{Fib}$CD34+). Thus, we decided to couple a first phase of "plastic" induction or de-differentiation by short-term exposure to iPSC reprogramming conditions[7,8], followed by MIM differentiation (Fig. 2a). First, we explored the suitability of this conversion process by retroviral approaches and the traditional four-factor combination, including *SOX2*, *Oct4*, *KLF4* and *c-Myc*, in two different lines of neonatal (HFF and BJ) as well as adult human dermal fibroblasts (HDF). 8-day exposure of human fibroblasts to reprogramming factors and iPSC-like culture conditions coupled to MIM differentiation for an additional 8-day period led to the appearance of a prominent $_{Fib}$CD34+ population (Fig. 2b, c). Additionally, we asked whether the miR 302–367 clusters, demonstrated to play a role during reprogramming towards iPSCs[17,18], could lead to increasing efficiencies of $_{Fib}$CD34+ cell generation. miR 302–367 seemed to contribute to the conversion of human fibroblasts in some but not all lines analyzed (Fig. 2c and Supplementary Fig. 7). MIM differentiation led to a significant upregulation of angioblast-related markers in all conditions analyzed (Fig. 2d). Sorting of MIM-differentiated $_{Fib}$CD34+ cells and subsequent differentiation into endothelial and smooth muscle cells resulted in the upregulation of lineage-specific markers at both the RNA and protein levels (Fig. 2e, f and Supplementary Fig. 7). We next sought to determine the minimal combination of factor(s) required for the conversion of human fibroblasts into $_{Fib}$CD34+ by systematic single factor removal. Marginal levels of CD34+ cells were found when *SOX2* was employed alone. Yet, subsequent differentiation of sorted *SOX2*-generated CD34+ cells did not result in the generation of endothelial nor smooth muscle cells. Altogether, the four Yamanaka factors, alongside the use of iPSC-like culture conditions, seemed indispensable for the conversion, into $_{Fib}$CD34+ with bi-potent differentiation potential resembling that of an angioblast-like state.

Similarly to PSC differentiation, cell fate conversion of human fibroblasts towards the endothelial lineage resulted in a mixture of different endothelial sub-types, including the expression of arterial, venous and lymphatic endothelial markers[19] (Supplementary Fig. 8). Along the same line, analysis of human fibroblasts converted to smooth muscle cell populations demonstrated mixed expression of smooth muscle markers[20] including expression of the pericyte marker NG2 (Supplementary Fig. 9). Of relevance, the converted endothelial cells had lost many features of the fibroblast profile and acquired characteristics of primary endothelial cells (Fig. 2g and Supplementary Fig. 5). Converted endothelial cells also lost their fibroblast epigenetic signature and acquired a DNA methylation profile that closely resembled that of primary endothelial cells (Fig. 2h and Supplementary Fig. 5). When all samples were compared, regardless of their method of derivation, fibroblasts formed a third major group in the differentiated portion of the dendograms, slightly closer to the primary and PSC-differentiated endothelial cell clusters as compared to converted endothelial cells, which clustered more closely to iPSC-differentiated cells. Interestingly,

both, the mRNA expression and DNA methylation results were very similar in terms of describing the relationships among all different cell types (Supplementary Fig. 5 and 6).

Altogether, our results demonstrate that 8-day exposure to iPSC reprogramming factors and culture conditions was sufficient for the induction of an intermediate plastic state in human fibroblasts. Further mesodermal induction by 8-day exposure to MIM yielded intermediate CD34+ bi-potent progenitor populations, which ultimately led to the generation of both endothelial and smooth muscle cell populations. Whereas expandable populations, alongside the lack of clonal expansion and colony formation, made precise frequency analysis technically difficult, "angioblast conversion efficiencies" could be calculated by estimating the ratio between the final number of converted cells and the initial number of fibroblasts. Taking into account that 75,000 fibroblasts give rise to ~2×10^6 cells by the end of MIM commitment, of which 20–60% are CD34+ (depending on the cell line of origin and the method used for plasticity induction), conversion efficiencies would range between 400–1200%. Altogether, human fibroblasts were subjected to three different steps during the process of conversion: first, a controlled phase of reprogramming totaling 8 days; second, specification of the generated reprogrammed intermediates to mesodermal $_{Fib}$CD34+ progenitor cells by MIM; lastly, further differentiation of the generated $_{Fib}$CD34+ cells to endothelial and smooth muscle cells.

Conversion to angioblasts by non-integrative approaches

We next wondered whether the process of conversion could result in an iPSC-like stage even in the absence of visible flattened ES-like colonies. We focused on TRA1-81 and TRA1-60 expression as the latter has been recently described as the most reliable early marker for iPSC generation, with a success prediction rate of up to 90%[21]. Plastic induction did not lead to the expression of either TRA1-60 or TRA1-81 (Fig. 2b and Supplementary Fig. 10).

Noticeably, residual expression of the transgenes was still detectable upon differentiation (Supplementary Fig. 10). In view of these results as well as the possibility for re-activation of integrated oncogenes, we next pursued the establishment of non-integrative approaches. To this end we evaluated an episomal vector combination proven to allow for the generation of human iPSCs in the presence of murine feeder layers[22]. A six-factor combination including *Oct4*, *SOX2*, *KLF4* and non-transforming *LMYC (MYCL1)* alongside shRNA-*p53* and *LIN28* was chosen for further experiments (Fig. 3). Plastic reprogramming intermediates were obtained by electroporation of 1.5 μg of DNA from each of the vectors followed by a 6-day resting phase prior to switching to iPSC-like reprogramming conditions (Fig. 3a). After 8 days, the media was changed to MIM, for an additional 8 days resulting, in the appearance of CD34+ cells whereas expression of TRA1-60 and TRA1-81 remained undetectable (Fig. 3b, c). Sorting of $_{Fib}$CD34+ cells and subsequent differentiation into endothelial and smooth muscle lineages resulted in the upregulation of cell-type specific markers at both the RNA and protein level (Fig. 3d–g). The generated endothelial and smooth muscle cells represented mixed populations of different sub-types similar to the results obtained by differentiation of PSCs (Fig. 3g).

Most importantly, we observed the rapid clearing of the episomal vectors and no random integration of exogenous genes was detected in the differentiated endothelial cells (Supplementary Fig. 10). Furthermore, testis injection of one million differentiated endothelial cells did not result in teratoma formation in any of the groups analyzed after 10 weeks, including cells generated by differentiation of PSCs (Supplementary Fig. 10).

Converted cells are functional *in vitro* and *in vivo*

Two well-characterized physiological hallmarks of smooth muscle cell function are their calcium responses as well as cell contraction capabilities[20,23,24]. Contraction of differentiated smooth muscle cells occurred both spontaneously as well as upon drug stimulation (Supplementary Fig. 11 and Supplementary Video 1). Exposure to carbachol resulted in rapid Calcium transients. Of note, whereas we did observe a response of 293T human embryonic kidney cells to carbachol, this response was limited to calcium transients and did not result in the physical contraction of the cells as demonstrated by their unchanged cell surface area (Supplementary Fig. 11). We next investigated the functionality of the generated endothelial cells by measuring their acetylated-LDL uptake, a characteristic of mature endothelial cells. CD34+-derived endothelial cells showed significantly higher rates of LDL uptake as compared to their respective negative controls (Fig. 3h and Supplementary Fig. 12). Noticeably, differentiated endothelial cells aggregated into vessel-like structures *in vitro* and were able to form functional vessels, allowing for blood circulation, after 17 days *in vivo* (Fig. 3i, 4 and Supplementary Fig. 12). Thus, demonstrating connection of the newly formed vessels to the pre-existing vasculature. Endothelial cell identity was verified by Ulex-lectin binding and the human origin of the cells further verified by *in situ* hybridization (Fig. 4b, c) as well as the use of antibodies specific for human CD31 and co-localization with the human nuclear antigen (Fig. 4d, e).

Altogether our results demonstrate that the use of chemically defined MIM media allowed for the commitment of plastic reprogramming intermediates to an angioblast-like fate. Further differentiation of angioblast-like cells resulted in the generation of functional endothelial and smooth muscle cells. Most importantly, 8-day reprogramming coupled to subsequent MIM differentiation for another 8 days was sufficient to drive the conversion of both neonatal and adult human fibroblasts to angioblast-like progenitor cells while bypassing iPSC generation. Lastly, PSC-derived as well as converted CD34+-derived endothelial cells demonstrated functionality *in vitro* and contributed to the vasculature *in vivo*.

DISCUSSION

We have established an efficient method for the conversion of human fibroblasts into CD34+ angioblast-like progenitor cells (Supplementary Table 1). These cells could be further differentiated into functional endothelial and smooth muscle cells. Interestingly, we observed certain differences at both the transcriptome and methylome level when compared to the positive controls. One possible explanation could reside in the unspecific nature of the generated endothelial and smooth muscle populations, including different sub-types of each respective major lineage as compared to the primary cells analyzed (Human Umbilical Vein

Endothelial Cells and Arterial Smooth Muscle Cells). Another explanation could be reminiscent to the epi/genetic differences found when comparing iPSCs versus ESCs, their respective positive "control", as well as when comparing different ESC clones[25]. Lastly, residual epigenetic marks from the initial fibroblast cells might also account for the observed differences[6]. Nevertheless, all the cells generated (either differentiated from PSCs or derived by conversion of human fibroblasts) demonstrated functional properties, thus, highlighting the potential of these novel conversion methodologies as well as the importance of analyzing functional parameters in reprogramming paradigms[6,25,26].

Conversion into angioblast-like progenitor cells occurred in the absence of iPSC colony formation, surface marker expression and re-activation of the endogenous transcription network regulating pluripotency, therefore shortening considerably the time required for generation of the desired cell types. Whereas the current measures do not permit us to rule out that converted cells transitioned through a somewhat "pluripotent-like" state, the lack of pluripotent marker expression and teratoma formation indicates that the conversion process does not result in the typical iPSC features. Furthermore, the fact that induction of "plasticity" relies on a first phase of epigenetic erasure, which by similarity with iPSC reprogramming might imply a stochastic process, strongly suggests that the heterogeneity observed at the molecular level during the conversion process might be due to the presence of cells with varying degrees of epigenomic plasticity. The present study represents the first demonstration that short-term induction by iPSC reprogramming conditions, followed by exposure to a chemically defined differentiation media, is sufficient for the conversion of neonatal and adult human fibroblasts into angioblast-like progenitor cells. Of note, not only the autonomous effects of the reprogramming factors but the overall combination of stem cell culture conditions promoting cell proliferation, as exemplified by the requirement of bFGF, have demonstrated to be crucial during the process of conversion in a similar way to iPSC reprogramming. Interestingly, culture conditions have also been highlighted as a critical component during the conversion process in similar reports[7,8]. Contrary to direct lineage conversion, that requires precise knowledge and screening of molecules defining target cell identity, induction of "plastic/de-differentiation" states coupled to specific differentiation protocols might provide a general, more readily accessible, platform towards the broader generation of clinically relevant cell types. Furthermore, whereas direct lineage conversion might be viewed as an "unnatural" process[6] occurring in the absence of progenitor cell generation, our results and those reported for the murine system[7,8] show, as during normal embryogenesis, the formation of intermediate progenitor states. Therefore, whereas direct lineage conversion occurs in one-to-one basics in the absence of progenitor cell generation and cell proliferation, transition through a proliferative progenitor state may have two major practical implications. On the one hand the generation of progenitor cells with multilineage differentiation capacity strongly diversifies the spectra of applications as opposed to direct lineage conversion. On the other hand, the inability to generate proliferative populations by direct lineage conversion could represent a major limitation for applications in which large numbers of cells are required[6,9]. Of note, in the case shown here, the conversion of human fibroblasts into vascular smooth muscle and endothelial cells proceeds through the generation of an expandable population of vascular progenitors with multilineage differentiation capacity. Altogether, our results describe a novel methodology

for the reprogramming of somatic cells and provide a complementary approach to those of direct lineage conversion and iPSCs methodologies for the generation of specific human cell types.

MATERIAL AND METHODS

Reagents and antibodies

The following antibodies were used at the specified concentrations: mouse anti-human CD34-APC 1:10 (130–046–703, Miltenyi), mouse anti-human CD133/2 (293C3)-PE 1:10 (130–090–853, Miltenyi), mouse anti-human CD144-PE 1:10 (VE-cadherin; 560410, BD biosciences), mouse anti-human CD144-APC 1:10 (VE-cadherin; 348507, Biolegend), CD105-PE 1:10 (endoglin; ab60902, Abcam), mouse anti-human CD105-PE 1:10 (endoglin; 560839, BD biosciences), CD31-FITC 1:10 (555445, BD biosciences), CD117-PeCy7 1:10 (c-Kit; 339195, BD biosciences), VEGFR2-PE 1:10 (KDR; 560494, BD biosciences), mouse anti-human CD45-FITC 1:10 (130–080–202, Miltenyi), anti-human CD235a-PE 1:10 (340947, BD biosciences), mouse APC isotype control 1:10 (555751, BD biosciences), mouse FITC isotype control 1:10 (555748, BD biosciences), PeCy7 isotype control 1:10 (557872, BD biosciences), PE isotype control 1:10 (555749, BD biosciences), VE-Cadherin 1:500 (555661, BD biosciences), Endoglin 1:500 (M3527, DAKO), Anti-von Willebrand Factor 1:200 (vWF; 7356, Millipore), calponin 1:500 (Dako, M3556), α-SMA 1:500 (AB56994, Abcam), α-SMA 1:1000 (A5228, Sigma), PECAM-1 (M-20) 1:100 (CD31; sc1506, Santa Cruz Biotechnology) anti-Human Nuclei 1:100 (MAB1281, Millipore), DAPI [5 mg ml^{-1}] 1:2000 (D1306, Invitrogen), Hoechst 33342 [5mg ml^{-1}] 1:2000 (B2261, Sigma), Alexa fluor 488 goat anti-mouse (A11001, Invitrogen), Alexa fluor 488 Donkey anti-goat (A11055, Invitrogen), Alexa fluor 568 Donkey anti-mouse (A10037, Invitrogen), Alexa-fluor 568 Donkey anti-rabbit (A10042, Invitrogen).

Cell culture

Human ES cells, H1 (WA1, WiCell), HuES 9 (http://www.mcb.harvard.edu/melton/hues/) and Human iPS cells CBiPS[27] and KiPS[28] (KIPS 4F#2, CBiPS 2F#4) (passage 25–45) were cultured in chemically defined hES/hiPS growth media (mTeSR[29] on growth factor reduced matrigel (35623, BD biosciences) coated plates). Briefly, 70–80% confluent hES/iPS cells were treated with dispase (Invitrogen) for 7 minutes at 37°C, colonies were dispersed to small clusters and lifted carefully using a 5 ml glass pipette, at a ratio of ~1:4. Neonatal human fibroblasts (HFF-1, BJ; ATCC) and adult human dermal fibroblasts (HDF-693) were cultured in DMEM containing 10% FBS, 2 mM GlutaMAX (Invitrogen), 50 U ml^{-1} penicillin and 50 mg ml^{-1} streptomycin (Invitrogen). Human Umbilical Vein Endothelial Cells (HUVEC) were purchased from Promocell and cultured in EBM medium supplemented with EGM-2 singlequots (cc-3162, Lonza), 2% FBS, hEGF 10 μg ml^{-1}, Heparin 100 μg ml^{-1} (Sigma). iPS/ES-derived endothelial cells were cultivated in EBM-2 medium supplemented with EGM-2 singleQuot kit (cc-3162, Lonza). iPS/ES-derived smooth muscle cells were cultured in SmBM medium supplemented with SmGM-2 singleQuot kit (cc-3182, Lonza). All the cells were grown in collagen I coated plates (BD biosciences). All cell lines were maintained in an incubator (37°C, 5% CO2) with media changes every day (hES/iPS) or every second day (HUVEC/Fibroblasts).

Directed differentiation of hES/hiPS cells in chemically defined conditions

Human ES/iPS cells cultured as described above were freshly split on matrigel-coated plates, making sure the sub-colonies were of small size (~300–500 cells/colony). After 24 hours of recovery in mTeSR, the cells were gently washed using DMEM:F12 (Invitrogen) and allowed to grow in chemically defined differentiation media (Mesodermal Induction Media or MIM), which consists of DMEM:F12, 15 mg ml^{-1} stem cell grade BSA (MP biomedicals), 17.5 µg ml^{-1} Human Insulin (SAFC bioscience), 275 µg ml^{-1} Human holo-transferrin (Sigma Aldrich), 20 ng ml^{-1} bFGF (Stemgent), 50 ng ml^{-1} Human VEGF-165 aa (Humanzyme), 25 ng ml^{-1} human BMP4 (Stemgent), 450 µM monothioglycerol (Sigma Aldrich), 2.25 mM each L-Glutamine and Non-essential amino acids (Invitrogen), systematically designed by titration of growth factors and culture conditions. Media was changed every second day with addition of half the volume of media every other day.

Single Cell Differentiation Assays

Upon MIM differentiation for 8 days, CD34+ Angioblast-like cells (Angioblast-like) were sorted and plated in collagen I coated 48-well plates at a density of one cell/well in either EBM-2 (endothelial differentiation) or SmBM (Smooth Muscle differentiation) supplemented as described above. After 7 days in the respective differentiation conditions cells were washed once with PBS and fixed with 4% Paraformaldehyde (PFA) in 1X PBS. Following fixation, cells were blocked and permeabilized for 1 hour at 37° C with 5% BSA/5% appropriate serum/1X PBS in the presence of 0.1% Triton X100. Subsequently, cells were incubated overnight at 4° C with an anti-endoglin antibody in case of cells in EBM-2/EGM-2 or with an anti-calponin antibody in the case of cells in SmBM/SmGM-2. Cells were then washed thrice with 1X PBS, incubated for 1 hour at 37° C with the respective secondary antibodies and 20 minutes with DAPI for nuclear staining. Following incubation, cells were washed thrice with 1X PBS before microscopy analysis and scoring.

Conversion of human fibroblasts into angioblast-like CD34+ progenitor cells

For retroviral infection, 75,000/well human fibroblast cells (HFF-1, BJ, HFF-693) were plated on matrigel-coated 6-well plates. The next day, cells were infected with an equal ratio of either a combination of 4 pMX-derived retroviruses encoding *Oct4*, *SOX2*, *KLF4* and *c-Myc* (4F) or 5 pMX-derived retroviruses encoding *Oct4*, *SOX2*, *KLF4*, *c-Myc* and miRs302–367 (4F/miRs). Scramble miRNA control (PMIRH000PA-1, SBI) was used whenever appropriate. The plates were infected by spinfection of the cells at 1850 rpm for 1 hour at room temperature in the presence of polybrene (4 µg ml^{-1}) and put back in the incubator without media change. 24 hours later, the media was switched to WiCell media composed of DMEM/F12 (Invitrogen), 20% Knockout serum replacement, 10 ng ml^{-1} bFGF, 1 mM GlutaMax, 0.1 mM non-essential amino acids and 55 µM β-mercaptoethanol; with media changes every day. After 6 days, cells were split at a ratio of 1:3 on to matrigel coated 6-well plates supplemented with WiCell media for another 2 days. The cells were then washed once with DMEM/F12 and induced for differentiation for 8 days in the presence of MIM. Media was changed every second day with addition of half the volume of media every other day.

For episomal transfection, 2.10^6 cells were transfected with 1.5μg each of pCXLE-episomal vectors encoding for *Oct4*, *SOX2*, *KLF4*, *LMYC*, *LIN28* and shRNA-p53[22] (#27077, #27078 and #27080, addgene) with and without addition of pcDNA3.1 encoding for miRs302–367 (6F or 6F/miRs). Fibroblasts were transfected by nucleofection (Amaxa NHDF nucleofector kit, # VPD-1001) according to manufacturer's instructions, and plated back on to matrigel-coated wells. After 6 days resting in DMEM/F12 supplemented with 10% FBS, 0.1 mM non-essential amino acids and 2 mM GlutaMAX, the media was switched to WiCell media with media changes every day. After 6 days, cells were split at a ratio of 1:3 on to matrigel coated 6-well plates with WiCell media for another 2 days. The cells were then washed once with DMEM:F12 and induced for differentiation for 8 days in the presence of MIM. Media was changed every second day with addition of half the volume of media every other day.

RNA isolation and real time-PCR analysis

Total cellular RNA was isolated using Trizol Reagent (Invitrogen) according to the manufacturer's recommendations. 2μg of DNAse1 (Invitrogen) treated total RNA was used for cDNA synthesis using the SuperScript II Reverse Transcriptase kit for RT-PCR (Invitrogen). Real-time PCR was performed using the SYBR-Green PCR Master mix (Applied Biosystems). The levels of expression of respective genes were normalized to corresponding GAPDH values and are shown as fold change relative to the value of the control sample. All the samples were done in triplicate. The list of the primers used for real time-PCR experiments are listed in Supplementary Table 3.

Flow cytometry analysis

Human ES/iPS cells undergoing directed differentiation, lineage converted CD34+ cells or their respectively derived endothelial cells were harvested using TripLE (Invitrogen), washed once with PBS and further incubated with the corresponding antibodies in the presence of FACS blocking buffer (1xPBS/10%FCS) for 1 hour on ice in the absence of light. After incubation, cells were washed thrice with 1 ml of FACS blocking buffer and resuspended in a total volume of 200 μl prior to analysis. A minimum of 10,000 cells in the living population were analyzed by using a BD LSRII flow cytometry machine equipped with 5 different lasers and the BD FACSDiva software. Percentages are presented after subtracting isotype background and referring to the total living population analyzed. Results are representative of at least three independent experiments with a minimum of two technical replicates per experiment.

Cell sorting

After 8 days of differentiation CD34+ cells were stained as described above and sorted by using a BDAria II FACS sorter (BD Biosystems). Alternatively, CD34+ cells were enriched using anti-CD34 conjugated magnetic beads (Miltenyi) according to the manufacturer's instructions with slight modifications. Briefly, up to 10^9 cells were incubated with constant mixing at 4°C with 100 μl of the corresponding magnetic beads in the presence of 100 μl of Fc-blocking solution in a total volume of 500 μl FACS blocking buffer. After 1 hour, cells were sorted by two consecutive rounds of column separation in order to increase purity by applying MACS separation magnets. Shortly, cells were passed through the first MS

separation column allowing binding of labeled cells. Non-labeled cells were washed thoroughly with 3 ml FACS blocking buffer prior to elution of the labeled fraction. Eluted labeled cells were then subjected to a second purification step as described above.

Differentiation of CD34+ cells to endothelial cells

PSC- and lineage converted-CD34+ cells, isolated by MACS or by FACS sorting after 8 days of differentiation in MIM, were plated in collagen I coated plates (50,000 cells well^{-1} of a 12 well plate) and cultured in EBM-2/EGM-2 (Lonza) with media changes every day. After 5–8 days in culture, upon reaching 90% confluence, cells were split 1:4, using TripLE (Invitrogen). The cells were cultured for at least 8 passages.

Differentiation of CD34+ cells to smooth muscle cells

PSC- and lineage converted-CD34+ cells, isolated by MACS or by FACS sorting after 8 days of differentiation in MIM, were plated in collagen I coated plates (50,000 cells well^{-1} of a 12-well plate) and cultured in SmBM/SmGM-2 (Lonza) with media changes every day. After 5–8 days in culture, upon reaching 90% confluence, cells were split 1:4, using TripLE (Invitrogen). The cells were cultured for at least 8 passages.

DNA Methylation Analysis

Illumina 450K Infinium Methylation Arrays were normalized and pre-processed in Genome Studio. Probes with missing values were removed. A filter for average Beta value difference between groups (PSCs, Fibroblasts, primary human Arterial Smooth Muscle Cells (PriSMC), primary human Umbilical Vein Endothelial Cells (PriEC), PSC → CD34+ Progenitor Cells, PSC → Endothelial Cells (iECs), converted Endothelial Cells (cECs), PSC → Smooth Muscle Cells (iSMCs), converted Smooth Muscle Cells (cSMCs)) of 0.3 was applied. The resulting probes were used for ANOVA analysis using R scripts with a p-value filter of <0.0001)(at this point, 30,000 probes remained). Probes with beta value difference of at least 0.3 ((max - min) >= 0.3) were used. ANOVA test (p<0.05; Var 0.58) was applied to obtain statistically significant differentially methylated probes among the 5 groups in both SMC and EC sample group. The resulting probes (see Supplementary Data) were used for hierarchical clustering using Cluster 3.0 with complete linkage. Venn Diagram Plotter (http://omics.pnl.gov/software/VennDiagramPlotter.php) was used to generate "area-proportional Venn Diagrams".

Gene Expression microarray analysis

The following groups were analyzed: PSCs, Fibroblasts, primary human Arterial Smooth Muscle Cells (PriSMC), primary human Umbilical Vein Endothelial Cells (PriEC), PSC → Endothelial Cells (iECs), converted Endothelial Cells (cECs), PSC → Smooth Muscle Cells (iSMCs) and converted Smooth Muscle Cells (cSMCs). Briefly, total RNA was extracted from collected sample pellets (Ambion mirVana; Applied Biosystems) according to the manufacturer's protocol. RNA quantity (Qubit™ RNA BR Assay Kits; Invitrogen) and quality (RNA6000 Nano Kit; Agilent) was determined to be optimal for each sample prior to further processing. 200ng RNA per sample was amplified using the Illumina® Total Prep™ RNA Amplification Kit according to manufacturer's protocol and quantified as above.

750ng RNA/sample was hybridized to Illumina HT-12v3 Expression BeadChips, scanned with an Illumina iScan Bead Array Scanner and quality controlled in GenomeStudio and the lumi bioconductor package. All RNA processing and microarray hybridizations were performed in-house according to manufacturer's protocols. Differential expression was defined as a minimum 2x fold-change and multiple-testing corrected p<0.05 by ANOVA. The resulting probes (see Supplementary Data) were used for hierarchical clustering using Cluster 3.0 with complete linkage. Probes with minimum gene expression differences between groups of 2× fold-change were obtained (see Supplementary Data). Venn Diagram Plotter (http://omics.pnl.gov/software/VennDiagramPlotter.php) was used to generate "area-proportional Venn Diagrams".

Determination of copy number by quantitative PCR

Briefly, total DNA was extracted using the Qiagen DNeasy Blood & Tissue kit (QIAGEN). The purity and quantity of DNA was measured using a NanoDrop 8000 spectrophotometer (Thermo Scientific), and then used as templates for absolute quantitation by qPCR assay[22]. The primers used are listed above and their amplification efficiencies, as well as specificity, were checked by performing standard curve and melting curve analyses.

Immunocytochemistry and fluorescence Microscopy

Briefly, cells were washed thrice with PBS and fixed using 4% PFA in 1X PBS. After fixation, cells were blocked and permeabilized for 1 hour at 37° C with 5% BSA/5% appropriate serum/1X PBS in the presence of 0.1% Triton X100. Subsequently, cells were incubated with the indicated primary antibody either for 1 hour at room temperature or overnight at 4° C. The cells were then washed thrice with 1X PBS and incubated for 1 hour at 37° C with the respective secondary antibodies and 20 minutes with DAPI or Hoechst 33342. Cells were washed thrice with 1X PBS before analysis. Sections were analyzed by using an Olympus 1X51 upright microscope equipped with epifluorescence and TRITC, FITC, and DAPI filters. Confocal image acquisition was performed using a Zeiss LSM 780 laser scanning microscope (Carl Zeiss Jena, Germany) with 20×, 40× or 63× immersion objectives.

Acetylated-LDL uptake assay and vascular tube-like structure formation assay

In short, 80% confluent endothelial cells derived from human ES/iPS cells were incubated with 10μg ml^{-1} Dil-Ac-LDL (L23380, Molecular Probes) for 3 hours in DMEM:F12. The cells were washed 3 times with PBS, dissociated using TripLE and analyzed by flow cytometry. Briefly, to assess the formation of capillary structures, a suspension of 4.10^5 cells ml^{-1} endothelial cells in the presence EBM-2/EGM-2 was prepared. Subsequently, 100 μl well^{-1} were dispensed on flat bottom 96 well plates coated with Matrigel (BD biosciences). Tube formation was observed after 24 hours of incubation and a minimum of three replicates per experiment analyzed.

Hematopoietic colony-forming assays

Hematopoietic clonogenic assays were performed in 35-mm low adherent plastic dishes (Stem Cell Technologies, Vancouver, BC, Canada) using 1.1 ml dish^{-1} of methylcellulose

semisolid medium (MethoCult H4434 classic, Stem Cell Technologies) according to the manufacturer's instructions. Briefly, enriched CD34+ cells were sorted and immediately plated at various densities: 1.5×10^3 ml^{-1}, 3×10^3 ml^{-1} and 6×10^3 ml^{-1}. All assays were performed in duplicate. After 21 days of incubation plates were analyzed for the presence of both, Colony-forming units (CFU) and Burst-forming units (BFU).

Animals

All murine experiments were conducted with approval of The Salk Institute Institutional Animal Care and Use Committee (IACUC). NOD.Cg-PrkdcscidIl2rgtm1Wjl/SzJ mice (or NOD-Scid IL2rγ null abbreviated as **NSG**; age, 7 weeks; weight, 20 g) were purchased from Charles River Laboratories, housed in air-flow racks on a restricted access area and maintained on a 12 hour light/dark cycle at a constant temperature (22 ±1°C).

Matrigel plug assay

Anaesthesia was induced using a mixture of Xylazine (Rompun® 2%, Bayer) at 10 mg kg^{-1} and Ketamine (Imalgene1000, Merial) at 100 mg kg^{-1} in NaCl at 0.9% *i.p* injected at a dose of 10 ml kg^{-1}. The animals' backs were shaved, swabbed with Hexomedine®. Prior injection, HUVECs, HUES9-, KiPS-, BJ 6F- and BJ 6F/miRs- derived endothelial cells were harvested using TripLE (invitrogen). A total of 1.10^6 cells were resuspended in 500 μl of cold matrigel (Matrigel basement membrane matrix from BD Biosciences adjusted to 9.8 mg ml^{-1} PBS) supplemented with 150 ng of bFGF. Cell and no cell containing matrigel solutions were then injected subcutaneously in the back of mice, carefully positioning the needle between the epidermis and the muscle layer. Seventeen days later, mice were sacrificed and the matrigel plugs were removed by a wide excision of the back skin, including the connective tissues (skin and all muscle layers).

Tissue processing/analyses

For immunohistochemistry (IHC), *in situ* hybridization (ISH) or immunofluorescence (IF) analysis, cell-containing implants with associated connective tissues were fixed with Accustain® (SIGMA) for 24 hours, dehydrated through an ethanol series and then processed for paraffin embedding before being sliced with a microtome. Slices from paraffin-embedded samples were stained with appropriate antibodies or probes. Alternatively, plugs were harvested and fixed with a 4% paraformaldehyde solution overnight at 4°, washed thrice in PBS and then incubated in a glucose solution (30%) for another 48 hours before being sliced (45μm) with a cryostat (Leica). Both methodologies were equally successful to identify neovasculature derived from human cells.

For IHC, slides were stained with an anti human-CD31 monoclonal antibody and then incubated with biotin-labeled secondary antibody followed by incubation with streptavidin-HRP (Ventana Roche).

For ISH, slides were hybridized according to the manufacturer's protocol with an Alu probe (780–2845, Ventana Roche) and then labeled with the *ISH iView Blue Detection* kit (760–092, Ventana Roche).

For IHC and ISH, images were then captured with a camera mounted on a light microscope (Nikon E-800).

For immunofluorescence assays, slides were stained with either rhodamine-labeled Ulex Europaeus Agglutinin I (UEA I, a marker for human endothelial cells from Vector Laboratories) or PECAM-1 (M-20) (CD31; sc1506, Santa Cruz Biotechnology) and anti-Human Nuclei 1:100 (MAB1281, Millipore) counterstained with DAPI. Images were captured with confocal microscopes (Zeiss, LSM 510 or LSM780).

Calcium live cell imaging

Subconfluent cells were washed with DMEM:F12 and incubated for 45 minutes with 1 μM Fluo-4/AM (Molecular Probes) in 0.5% BSA, DMEM:F12 in an incubator at 37 °C, 95% CO_2. After washing to remove unloaded dye, cells responses to 100 μM carbachol or vehicle (water) were imaged in HEPES-buffered, phenol red-free DMEM:F12 in a wide field fluorescent microscope (Olympus BX61WI) equipped for fast fluorescent imaging. Image capture was performed with Metamorph and an EM-CCD camera (Hamamatsu). Image analysis was carried out with Metamorph and Fiji software. To determine functional SMC contraction after stimulations, the cell surface area was determined before and after carbachol exposure.

Statistical evaluation

Statistical analyses of all endpoints were performed by using standard unpaired Student t test (one-tailed, 95% confidence intervals) using the SPSS/PC + statistics 11.0 software (SPSS Inc.). All data are presented as mean ± standard deviation (s.d.) or standard error of the mean (s.e.m.) where indicated and represent a minimum of two independent experiments with at least two technical duplicates.

Supplementary Material

Refer to Web version on PubMed Central for supplementary material.

Acknowledgments

REFERENCE LIST

1. Sancho-Martinez I, Nivet E, Izpisua Belmonte JC. The labyrinth of nuclear reprogramming. J Mol Cell Biol. 2011; 3:327–329. [PubMed: 22090451]

2. Takahashi K, Yamanaka S. Induction of pluripotent stem cells from mouse embryonic and adult fibroblast cultures by defined factors. Cell. 2006; 126:663–676. [PubMed: 16904174]

3. Laiosa CV, Stadtfeld M, Xie H, de Andres-Aguayo L, Graf T. Reprogramming of committed T cell progenitors to macrophages and dendritic cells by C/EBP alpha and PU.1 transcription factors. Immunity. 2006; 25:731–744. [PubMed: 17088084]

4. Ieda M, et al. Direct reprogramming of fibroblasts into functional cardiomyocytes by defined factors. Cell. 2010; 142:375–386. [PubMed: 20691899]

5. Vierbuchen T, et al. Direct conversion of fibroblasts to functional neurons by defined factors. Nature. 2010; 463:1035–1041. [PubMed: 20107439]

6. Vierbuchen T, Wernig M. Direct lineage conversions: unnatural but useful? Nat Biotechnol. 2011; 29:892–907. [PubMed: 21997635]

7. Efe JA, et al. Conversion of mouse fibroblasts into cardiomyocytes using a direct reprogramming strategy. Nat Cell Biol. 2011; 13:215–222. [PubMed: 21278734]

8. Kim J, et al. Direct reprogramming of mouse fibroblasts to neural progenitors. Proc Natl Acad Sci U S A. 2011; 108:7838–7843. [PubMed: 21521790]

9. Sancho-Martinez I, Baek SH, Izpisua Belmonte JC. Lineage conversion methodologies meet the reprogramming toolbox. Nat Cell Biol. 2012; 14:892–899. [PubMed: 22945254]

10. Papp B, Plath K. Reprogramming to pluripotency: stepwise resetting of the epigenetic landscape. Cell Res. 2011; 21:486–501. [PubMed: 21321600]

11. Plath K, Lowry WE. Progress in understanding reprogramming to the induced pluripotent state. Nat Rev Genet. 2011; 12:253–265. [PubMed: 21415849]

12. Goldman O, et al. A boost of BMP4 accelerates the commitment of human embryonic stem cells to the endothelial lineage. Stem Cells. 2009; 27:1750–1759. [PubMed: 19544443]

13. Dzierzak E, Speck NA. Of lineage and legacy: the development of mammalian hematopoietic stem cells. Nat Immunol. 2008; 9:129–136. [PubMed: 18204427]

14. Choi KD, et al. Hematopoietic and endothelial differentiation of human induced pluripotent stem cells. Stem Cells. 2009; 27:559–567. [PubMed: 19259936]

15. James D, et al. Expansion and maintenance of human embryonic stem cell-derived endothelial cells by TGFbeta inhibition is Id1 dependent. Nat Biotechnol. 2010; 28:161–166. [PubMed: 20081865]

16. Levenberg S, Ferreira LS, Chen-Konak L, Kraehenbuehl TP, Langer R. Isolation, differentiation and characterization of vascular cells derived from human embryonic stem cells. Nat Protoc. 2010; 5:1115–1126. [PubMed: 20539287]

17. Anokye-Danso F, et al. Highly efficient miRNA-mediated reprogramming of mouse and human somatic cells to pluripotency. Cell Stem Cell. 2011; 8:376–388. [PubMed: 21474102]

18. Subramanyam D, et al. Multiple targets of miR-302 and miR-372 promote reprogramming of human fibroblasts to induced pluripotent stem cells. Nat Biotechnol. 2011; 29:443–448. [PubMed: 21490602]

19. Narazaki G, et al. Directed and systematic differentiation of cardiovascular cells from mouse induced pluripotent stem cells. Circulation. 2008; 118:498–506. [PubMed: 18625891]

20. Cheung C, Bernardo AS, Trotter MW, Pedersen RA, Sinha S. Generation of human vascular smooth muscle subtypes provides insight into embryological origin-dependent disease susceptibility. Nat Biotechnol. 2012; 30:165–173. [PubMed: 22252507]

21. Chan EM, et al. Live cell imaging distinguishes bona fide human iPS cells from partially reprogrammed cells. Nat Biotechnol. 2009; 27:1033–1037. [PubMed: 19826408]

22. Okita K, et al. A more efficient method to generate integration-free human iPS cells. Nat Methods. 2011; 8:409–412. [PubMed: 21460823]

23. Ohta T, Ito S, Nakazato Y. All-or-nothing responses to carbachol in single intestinal smooth muscle cells of rat. Br J Pharmacol. 1994; 112:972–976. [PubMed: 7921627]

24. Kohda M, Komori S, Unno T, Ohashi H. Carbachol-induced [Ca2+]i oscillations in single smooth muscle cells of guinea-pig ileum. J Physiol. 1996; 492 (Pt 2):315–328. [PubMed: 9019532]

25. Yamanaka S. Induced pluripotent stem cells: past, present, and future. Cell Stem Cell. 2012; 10:678–684. [PubMed: 22704507]

26. Yusa K, et al. Targeted gene correction of alpha1-antitrypsin deficiency in induced pluripotent stem cells. Nature. 2011; 478:391–394. [PubMed: 21993621]

27. Giorgetti A, et al. Generation of induced pluripotent stem cells from human cord blood using OCT4 and SOX2. Cell Stem Cell. 2009; 5:353–357. [PubMed: 19796614]

28. Aasen T, et al. Efficient and rapid generation of induced pluripotent stem cells from human keratinocytes. Nat Biotechnol. 2008; 26:1276–1284. [PubMed: 18931654]

29. Ludwig TE, et al. Derivation of human embryonic stem cells in defined conditions. Nat Biotechnol. 2006; 24:185–187. [PubMed: 16388305]
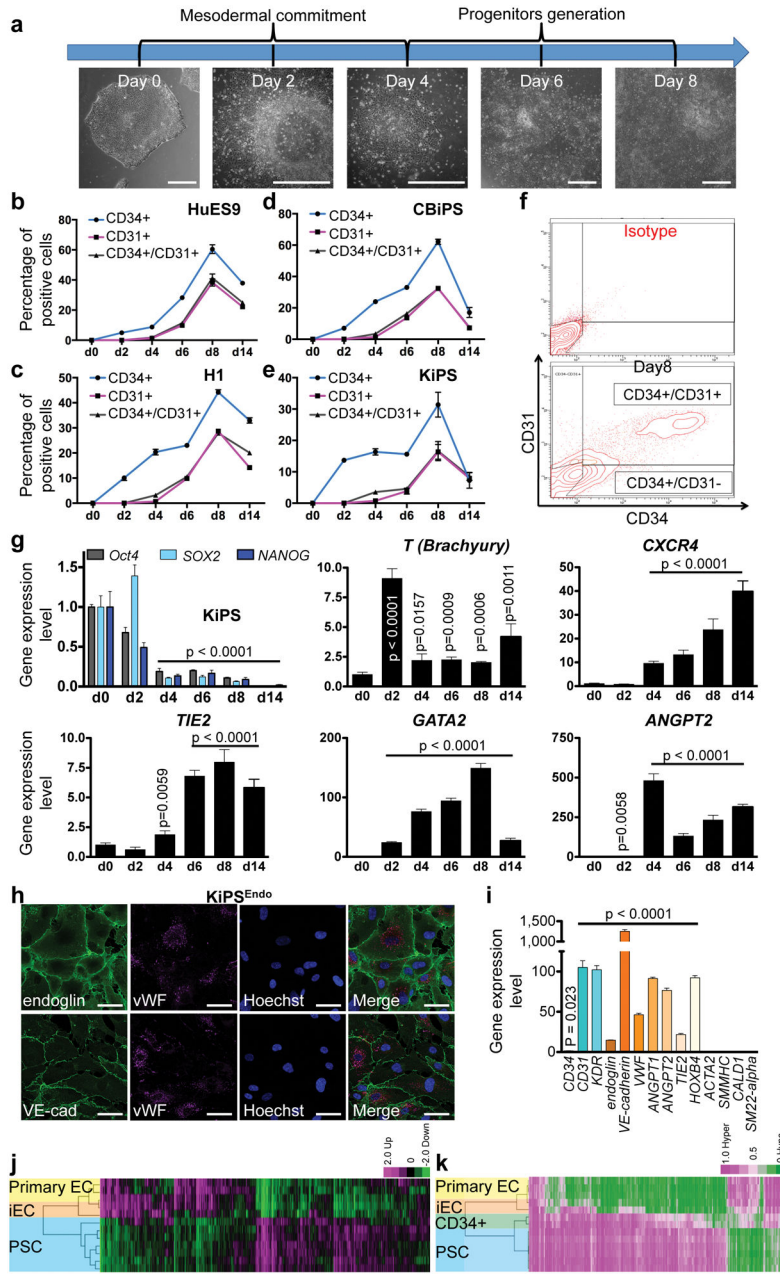
Figure 1. Differentiation of hPSCs into mesodermal progenitor and terminally differentiated endothelial cells

a) Scheme and Representative bright field pictures during the course of differentiation of human pluripotent stem cells towards CD34+ progenitor cells. **b–e**) Flow cytometry analysis of the mesoderm markers CD34 and CD31 over the differentiation course on HuES9 embryonic stem cells (**b**), H1 embryonic stem cells (**c**), two-factor cord blood-derived iPS cells (CBiPS) (**d**) and four factor keratinocyte-derived iPS (KiPS) (**e**). Representative flow cytometry plots depicting a double CD34+CD31+ population obtained after 8 days of PSC differentiation in the presence of Mesodermal Induction Media (MIM). Upper panel shows isotype controls. Lower panel shows specific CD34 and CD31 staining (**f**). **g**) mRNA fold-

change of pluripotency and mesodermal markers on KiPS. **h**) Fluorescence microscopy analysis showing the expression of indicated endothelial cell markers in KiPS derived Endothelial Cells (KiPS^{Endo}). **i**) mRNA expression profile showing specific upregulation of endothelial markers in KiPS^{Endo}. **j–k**) Heat-map and representative clustering of hPSCs as compared to induced/differentiated endothelial (iECs) as well as a representative primary endothelial cell line (Human Umbilical Vein Endothelial Cells; HUVEC). On the left, genome-wide transcriptome analysis results demonstrate high similarities between PSC-differentiated and primary endothelial cells (**j**). On the right, genome-wide methylation profiling representing the epigenetic changes occurring upon differentiation of PSCs into endothelial cells (iECs). Generated endothelial cells cluster closely to primary endothelial cells (**k**). See Supplementary Table 2 for specific gene-expression changes as summarized in the main figure panels. Error bars, s.d. Scale bars: 200 μm (**a**), 50μm (**h**). Endoglin and VE-cadherin stainings are depicted in green; vWF stainings are depicted in magenta; Nuclear stainings are depicted in blue.
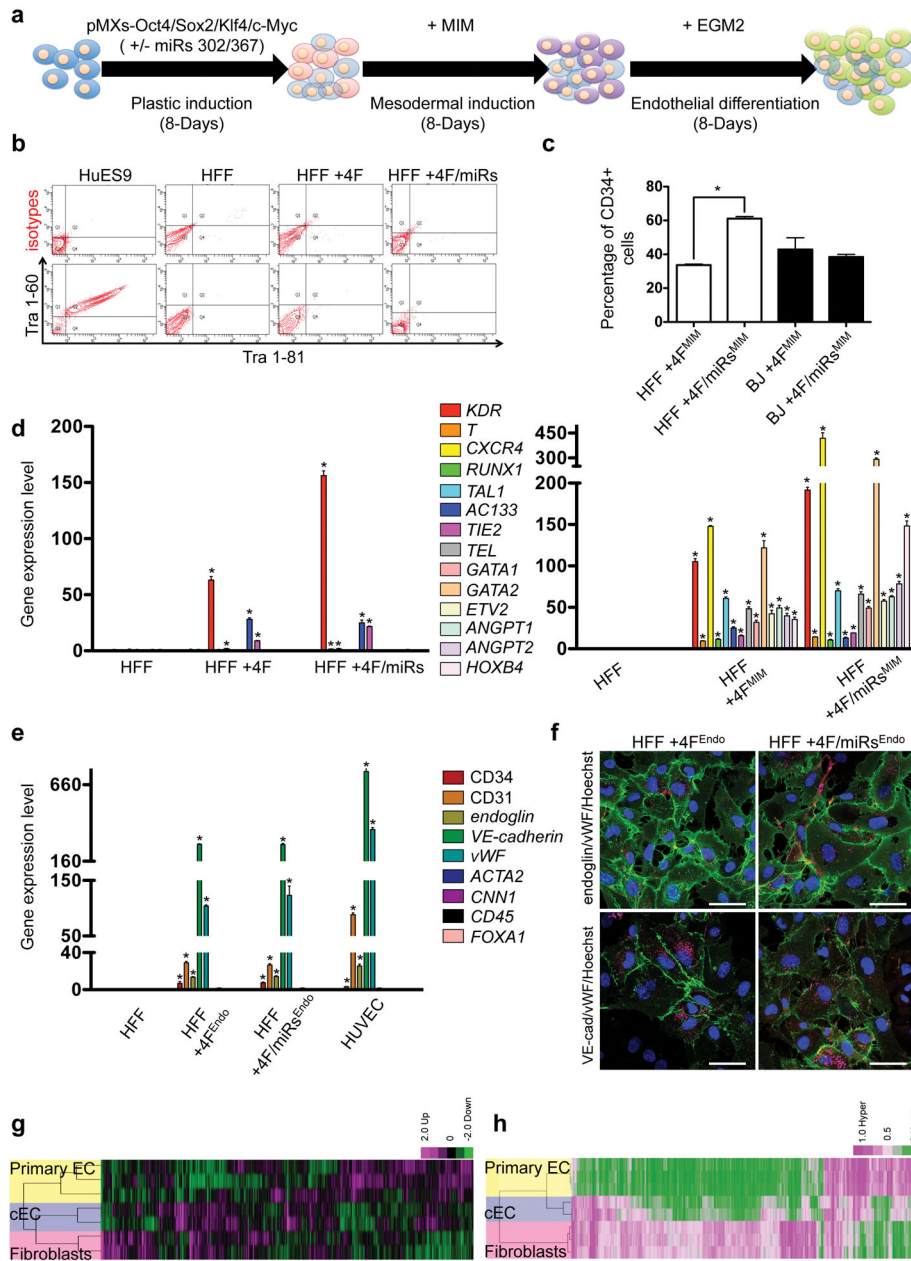
Figure 2. Conversion of human fibroblasts into mesodermal progenitor and terminally differentiated endothelial cells by retroviral approaches

a) Schematic representation of the conversion process towards CD34+ progenitor cells and further differentiation into terminally differentiated endothelial cells. **b**) Representative flow cytometry plots demonstrating absent expression of pluripotency-associated markers upon plastic induction followed by Mesodermal Induction Media (MIM) differentiation. **c**) Flow cytometry analysis of CD34 expression after MIM induction in neonatal human fibroblasts in the presence of miR302-367 or the respective scramble controls. **d**) mRNA expression profiling of mesodermal genes upon the first phase of "plastic induction" (left panels); mRNA expression profiling of mesodermal genes upon "plastic induction" followed by MIM differentiation (right panels). Note the significant upregulation of all mesodermal and

angioblast-related markers upon MIM exposure. **e**) mRNA expression profile showing specific upregulation of Endothelial Cell (EC) markers upon specific differentiation of sorted $_{Fib}$CD34+ cells into "converted" ECs. **f**) Fluorescence microscopy analysis showing the expression of the indicated endothelial markers in converted cells. **g–h**) Heat-map and representative clustering of the initial fibroblasts population as compare to converted $_{Fib}$CD34+ cells, endothelial cells (cECs) and a representative primary endothelial cell line (Human Umbilical Vein Endothelial Cells; HUVEC). On the left, genome-wide transcriptome analysis results demonstrating high similarities between converted and primary endothelial cells (**g**). On the right, genome-wide methylation profiling representing the epigenetic changes occurring upon conversion into converted endothelial cells. Converted endothelial cells (cECs) cluster closely to primary endothelial cells (**h**). See Supplementary Table 2 for specific gene-expression changes as summarized in the main figure panels. Scale bars: 50μm (**f**). Error bars, s.d. *P<0.05. Endoglin and VE-cadherin stainings are depicted in green; vWF stainings are depicted in magenta; Nuclear stainings are depicted in blue.
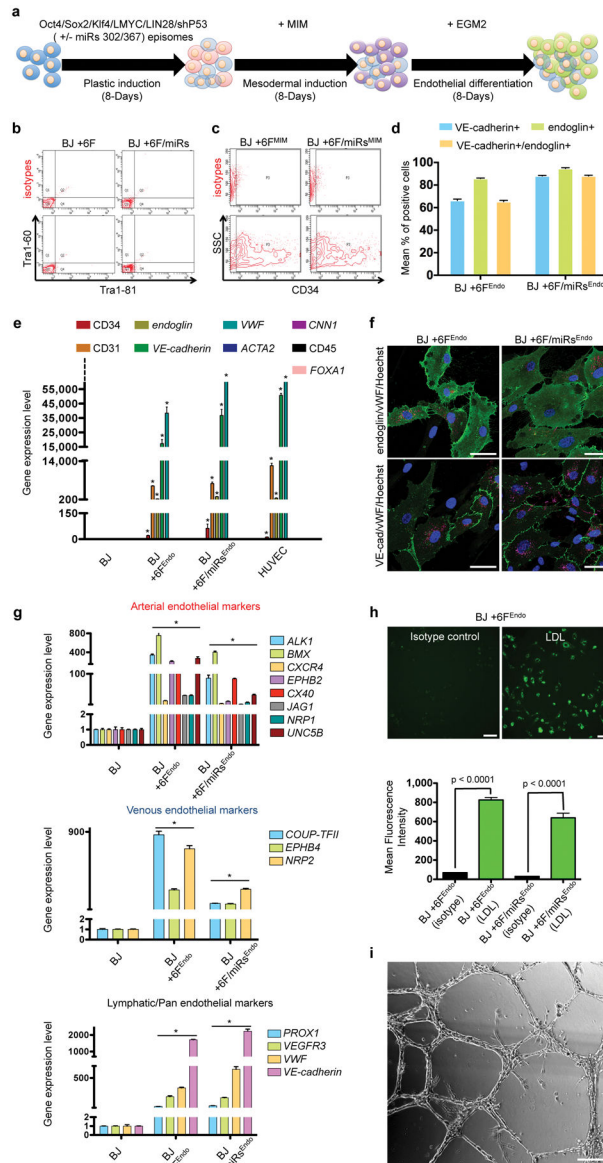
Figure 3. Conversion of human fibroblasts into mesodermal progenitor and terminally differentiated endothelial cells by non-integrative approaches

a) Schematic representation of the conversion process towards CD34+ progenitor cells and further differentiation into terminally differentiated endothelial cells. **b**) Representative flow cytometry plots demonstrating absent expression of pluripotency-associated markers upon plastic induction with non-integrative plasmids followed by Mesodermal Induction Media (MIM) differentiation. **c**) Representative flow cytometry analysis of CD34 expression before and after MIM differentiation in human fibroblasts (BJ) induced to a plastic state by the use of non-integrative approaches in the presence of miR302-367 or respective scramble controls. Upper panel shows isotype controls. Lower panel shows specific CD34. **d**) Representative flow cytometry quantification of BJ-converted VE-cadherin+ and endoglin+ endothelial cells derived in the presence of miR302/367 or respective scramble controls. **e**)

mRNA expression profile showing specific upregulation of endothelial markers upon specific differentiation of sorted BJ $_{Fib}$CD34+ cells into "converted" endothelial cells. **f**) Fluorescence microscopy analysis showing the expression of the indicated endothelial markers in converted cells. **g**) Characterization of endothelial subtypes in BJ converted endothelial cells. Note the mixed expression of different endothelial subtype markers including arterial, venous and lymphatic upon conversion of fibroblasts. **h**) Representative pictures of endothelial cells derived by non-integrative approaches upon LDL uptake as compared to the respective controls (upper panels). LDL Mean Fluorescence Intensities of BJ-derived endothelial cells that were converted by non-integrative approaches (lower panels). Controls represent converted endothelial cells in the presence of Alexa Fluor 488 in order to measure unspecific fluorescence background. **i**) BJ-derived endothelial cells converted by non-integrative approaches spontaneously formed capillary-like structures *in vitro*. See Supplementary Table 2 for specific gene-expression changes as summarized in the main figure panels. Scale bars: 50 μm (**f**); 100μm (**h**); 200μm (**i**). Error bars, s.d. *$P<0.05$. Endoglin and VE-cadherin stainings are depicted in green; vWF stainings are depicted in magenta; Nuclear stainings are depicted in blue.
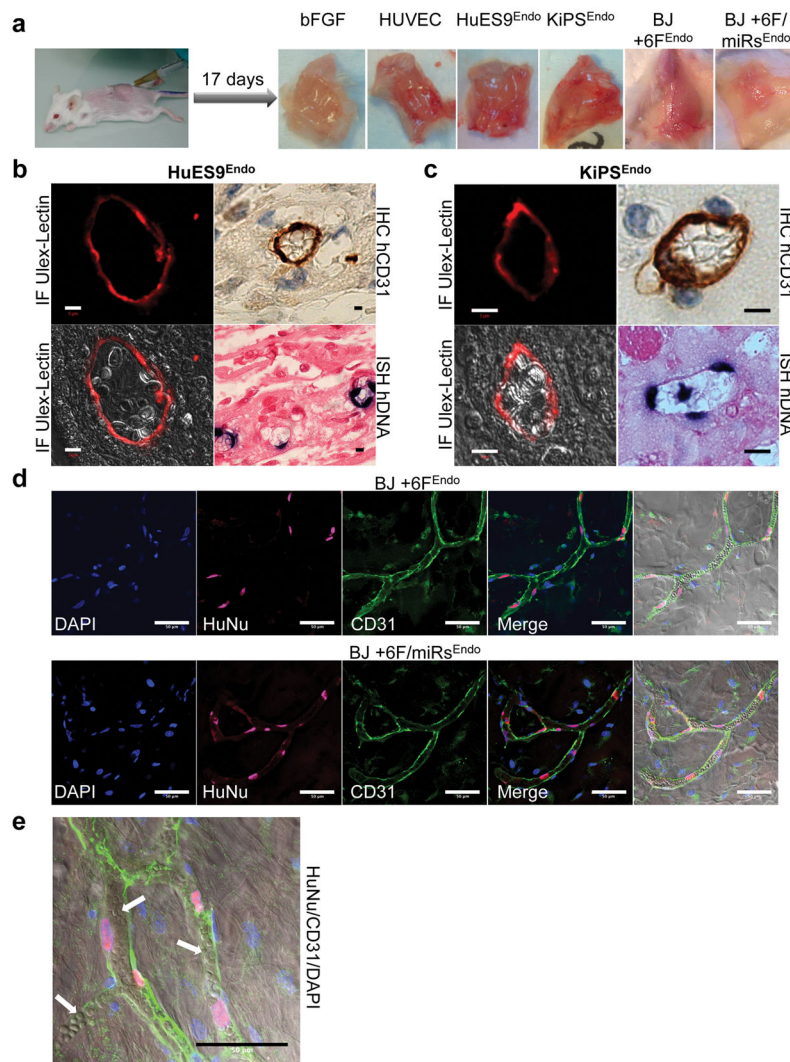
Figure 4. Generated Endothelial cells demonstrate functionality *in vivo*
a) 17 days after injection, matrigel plugs were extracted and processed for analyses. Pictures show increased blood circulation through the extracted plugs, thus demonstrating connection with the pre-existing vasculature (anastomosis) *in vivo*. **b, c**) Representative pictures of HuES9- (left panels) and KiPS- (right) derived endothelial cells showing the identification of human cells by *in situ* hybridization on ALU+ sequences (dark blue dot), anti-human CD31 staining (brown) and Ulex Lectin rhodamine staining (red). Note the presence of circulating red blood cells through the vessel-graft. **d**) Endothelial cells derived by non-integrative approaches-mediated conversion of human fibroblasts demonstrate anastomosis *in vivo*. Human specific CD31 antibody demonstrates the presence of converted endothelial cells (green). Co-localization with specific Human Nuclear Antigen staining demonstrates that the generated vessels are derived from the injected converted human endothelial cells. **e**) Representative high magnification picture demonstrating connection to the pre-existing vasculature upon injection of converted endothelial cells generated by non-integrative approaches. White arrows indicate the presence of circulating red blood cells. Scale bars: 5

μm (**b, c**); 50μm (**d, e**). CD31 stainings are depicted in green; Human Nuclear Antigen (HuNu) stainings are depicted in magenta; Nuclear stainings are depicted in blue.